The Thesis Committee for Karl A. Burkhardt
certifies that this is the approved version of the following thesis:

A Comparative Study of Entrainment in Supersonic Beams

Committee:

Mark G. Raizen, Supervisor

Greg O. Sitz

A Comparative Study of Entrainment in Supersonic Beams

by

Karl A. Burkhardt, B.S.

Thesis

Presented to the Faculty of the Graduate School of

The University of Texas at Austin

in Partial Fulfillment

of the Requirements

for the Degree of

Master of Arts

The University of Texas at Austin

August 2016

To my faithful family and my wonderful wife

Acknowledgments

I must first convey my appreciation to Mark Raizen. He was willing to give me an opportunity to perform research in his lab where I learned so much. Mark has taught me to think differently about problems which has in turn lead to experimental improvements that are measured in leaps and bounds and has made me a more successful scientist as well as a better problem solver in life.

Rodrigo Castillo-Garza and Jianyong Mo were the post-docs I had the pleasure of working with for the majority of my time in the Raizen Lab. Rodrigo passed on his knowledge of high current circuitries, which helped greatly while implementing the pulsed ribbon experiment. Jianyong taught me a great deal about how to run an experiment and keep it moving, even when it felt like everything was breaking.

I owe a lot to the fellow graduate students who worked on the Keck Foundation project with me. Kevin Melin wrote the LabView code that ran the experiments in this thesis and saved me many a headache by pointing out simple oversights in my heat pipe and pulsed ribbon designs; Yu Lu helped with circuit diagnostics in the pulsed ribbon experiment and constructed the magnetic slower which will be used in future experiments; Lukas Gradl helped with constructing the heat pipe and running the pulsed ribbon experiments;

and Isaac Chavez helped to design the circuitry for the pulsed ribbon experiments.

I am grateful for the company and consultation of the rest of the graduate students in the Raizen Lab as well. Jamie Gardner, Erik Anciaux, Georgios Stratis, and Igal Bucay were all there to talk about new experimental ideas, discuss how awful a football game Georgia Tech had just played, or share coffee with and vent about vacuum and electronic issues.

I also had the pleasure of working with Tharon Morrison, David Dunsky, and Alec Eickbusch during their time as undergraduate students in the Raizen Lab. I learned a lot from them and can only hope that I passed on as much information as I received.

My family has been instrumental in shaping me into who I am today and for that I am extremely grateful. My parents, grandparents, and sister have always encouraged me to pursue a good education and be the best that I can be. I am lucky enough to have married into another great family that has also been extremely supportive.

Finally, my wife Jennifer Burkhardt has helped to keep me sane through my time in graduate school. She didn't complain when I worked strange hours and was always there for me when I needed to vent. Coming home to her and our cats was always enough to brighten whatever kind of day I had been having.

Karl A. Burkhardt

The University of Texas at Austin

August 2016

A Comparative Study of Entrainment in Supersonic Beams

Karl A. Burkhardt, M.A.
The University of Texas at Austin, 2016

Supervisor: Mark G. Raizen

In the field of atomic physics, there is a growing demand for large numbers of dense, trapped atoms. The traditional method of generating trapped atoms is through laser cooling, however the field has reached saturation in terms of cold atom flux and phase-space density and is fundamentally limited to atoms that can be addressed using a two-level transition accessible with available lasers. Because of this a new, more general technique of generating dense clouds of trapped atoms is necessary. This technique will surpass laser cooling with higher cold atom flux and phase-space density, as well as be applicable to particles which cannot be put into a two-level system.

This thesis explores the first step necessary for the generation of a new method of cooling which will be more general than laser cooling and will pro-

duce a higher cold atom flux in denser phase-space. This method of cooling will rely on the sympathetic cooling of vaporized particles with a pulsed supersonic beam before slowing the entrained particles to rest using magnetic fields. Because the cooling in the entrainment step relies on sympathetic cooling, there is no two-level requirement and thus it is applicable to all paramagnetic species including both atoms and molecules.

The experiments outlined in this thesis focus on utilizing different methods of entraining vaporized atoms into a supersonic beam as an alternative method of generating cold atoms. A comprehensive comparison of entrainment efficiency using these different entrainment techniques is included as well as a discussion regarding future applications of this new cooling process.

Contents

List of Tables

List of Figures

Chapter 1

Introduction

Scientists have been studying atoms and their properties since the 17th century [1], however, it has only been in the last quarter century that scientists have been able to utilize atoms and their properties as tools. The purposes served by these atoms have varied greatly, ranging from atom lasers [2, 3], atomic clocks [4] and atom interferometers [5, 6], to measuring fundamental constants [7] and searching for gravity waves [8]. In addition to using atoms as tools, scientists have recently been able to use atomic physics experiments for the purpose of studying other systems such as superfluidity [9, 10] and condensed-matter and many body physics [11, 12], as well as observing thermodynamic principles in their most elementary form [13].

Although these recent results are extremely encouraging, there is a major limitation in their scalability. In order to scale these experiments, cold atom flux must be increased drastically. Currently, cold atom flux is limited by the very method used to generate cold atoms, laser cooling [14]. This means that a fundamentally new method of cooling is necessary to progress past the current limitation. The work outlined in this thesis aims to remove

this fundamental limitation by finding the most efficient method of entraining hot atoms into cold supersonic beams; the first step in realizing a new method of cooling.

1.1 The Need for Cold Atoms

Many cold atom experiments have been performed in the last quarter century that give encouraging results regarding future practical applications including atoms interferometers for purposes of position, navigation, and timing [5, 11, 15, 16], and trapped atom quantum bits for quantum computing [17, 18]. In addition to these applications, cold atoms can be used as an atom laser which was heralded as the next great lithography tool [2, 3].

Unfortunately however, the hype surrounding the lithography machine died down due to the small size of the Bose-Einstein condensates (BEC's) that are required to produce the laser. Because of this, research in the field has largely come to halt, although the capability to produce larger condensates would likely kindle newfound interest.

In addition to lithography applications, a higher flux of cold atoms would have a drastic effect on many other active areas of research, including areas which require the loading of optical lattices and optical tweezers where loading fidelity would be increased [19]. A higher flux of atoms would also benefit experiments such as tests of the weak equivalence principal [20, 21] and even gravitational wave detection [22, 23].

1.1.1 A Case Study - The Atom Laser

Because traditional optical lithography techniques are limited by the Rayleigh limit to half the wavelength of light used [24, 25], there has been a recent push to find new lithography sources which have shorter wavelengths [26]. Atoms have come to the forefront as possible replacement candidates for traditional visible lithography techniques because of their shorter de Broglie wavelengths [27].

Although atomic sources are able to be focused to a smaller spot size than visible light due to their shorter wavelengths, the atoms must be cooled to form a more coherent beam leading to a focal spot with minimal aberration [28, 29]. Ideally, atoms would be Bose condensed before being used as lithography tools to achieve optimal focusing [30].

The problem with using a BEC as a lithography tool is that there is a limited number of atoms in a BEC. Because the generation of BEC's rely on evaporative cooling, which is an inherently destructive technique to a large number of the originally trapped atoms, the resulting condensate onlt has a small fraction of the atoms which were initially trapped. For example, a typical BEC resulting from the evaporative cooling of a cloud of laser cooled and trapped atoms will be smaller in number by a factor of approximately 1,000 [31].

A new method of cooling which could trap a larger cloud of atoms prior to evaporative cooling would have two distinct advantages. The first advantage would be a larger cloud of trapped atoms prior to evaporative cooling, resulting

in a larger condensate. As can be seen in Eq. 1.1

$$\frac{T(t)}{T_o} = \left(\frac{N(t)}{N_o}\right)^{\alpha} \tag{1.1}$$

where T_o and $T(t)$ are the original and time-dependent temperatures of the cloud, N_o and $N(t)$ are the original and time-dependent number of atoms in the cloud, and α is a unit-less factor determined by the rate of cooling [31], starting with a larger value of N_o would result in a larger or colder condensate at a time t after evaporation.

The second advantage arises from the fact that atoms are not trapped in a perfect vacuum; since there is a non-negligible background pressure in the chamber, collisional heating is a significant source of loss in many experiments [32]. Eq. 1.1 assumes no external heating over the duration of the evaporative cooling process, but the reality is that the longer the cooling process takes, the more atoms are lost due to collisional background heating. By starting the evaporative cooling process with a larger number of atoms in the same space, cooling is a faster process resulting in less heating due to background pressure.

With a sufficiently brighter source of trapped atoms, evaporative cooling would be a faster, more efficient process which would result in larger, denser condensates [31]. These condensates would in turn have more atoms for use in lithography applications, overcoming the issue of weak flux that caused research in the field to stop.

A brighter source of trapped atoms would lead to a larger condensate with which to perform atom lithography. By improving the cold atom flux used to generate these BEC's, atom lasers would have high enough flux to realize their full potential as lithography tools.

1.2 Current Methods of Cold Atom Generation

As previously mentioned, scientists are already able to generate cold atoms using a variety of methods, the most common of which is laser cooling [14, 18]. Another popular technique is sympathetic cooling which has been used to cool particles which are difficult to address using commercially available lasers [33, 34, 35]. The basic principles of each method and their advantages and shortcomings are discussed below.

1.2.1 Laser Cooling

Laser cooling relies on the scattering of multiple photons where, on average, each scattering event removes energy from the atom. This process is continued until the atom reaches its Doppler limit

$$T_D = \frac{\hbar\gamma}{2k_B} \tag{1.2}$$

where T_D is the Doppler limit in Kelvin, $\hbar$ is the reduced Planck constant, γ is the natural linewidth of the radiative transition, and k_B is the Boltzmann constant [36]. At this limit, cooling reaches a steady state where the heating and cooling rates due to scattered photons are equal.

Although there are other methods of cooling which can be applied to the atoms such as resolved sideband [37], Sisyphus [38], or evaporative cooling [39], the initial laser cooling step, Doppler cooling, is fundamentally limited to T_D. In addition to having a temperature limit, Doppler cooling also has a density limit of 10^9 atoms/cm^3 [40]; because the cooling process is dependent

on scattered photons, a dense enough cloud of atoms will eventually disperse due to internal radiation pressure [14].

In addition to these limitations, laser cooling is only applicable to species with an accessible two-level transition. Even for atoms with true two-level transitions that do not require repump lasers such as hydrogen, laser cooling can be extremely difficult due to the complex laser systems required [41, 42].

For the vast majority of species however, there is no two-level transition which would not require repump lasers. The majority of atoms require repump lasers for laser cooling while all molecules require repump lasers, increasing experimental complexity [43, 44].

1.2.2 Sympathetic Cooling

The second most popular method of generating cold atoms is sympathetic cooling. Many different schemes have been developed ranging from cooling trapped ions with magneto-optically trapped atoms [45] and other trapped ions [46] to using a buffer gas to cool molecules [47, 48].

Rather than being limited to a temperature inherent to the species being cooled like the linewidth of a radiative transition in laser cooling, sympathetic cooling is limited only to the temperature of the cooling species [49]. Many different species have been used to sympathetically cool target particles, even vacuum chambers walls have been used to sympathetically cool hydrogen prior to Bose-Einstein condensation [50, 51]. The most important factors in determining a species for sympathetic cooling are a low ratio of inelastic to elastic collisions and a low initial temperature [47, 49].

Fortunately, noble gases meet both of these requirements and are good sympathetic cooling candidates. Noble gases are unlikely to interact inelastically with other atoms or molecules and therefore have a low ratio of inelastic to elastic collisions, and are able to be cooled to low temperatures before condensing. In addition, supersonic beams composed of noble gases have many favorable properties which make them ideal for sympathetically cooling entrained particles.

For a small number of target particles relative to carrier gas particles, the temperature ratio of the target species to the carrier gas is

$$\frac{T_M(l)}{T_m} = \left(\frac{T_M(0)}{T_m} - 1\right) e^{-l/\kappa} + 1 \tag{1.3}$$

where $T_M(0)$ and $T_M(l)$ are the temperatures of the target species after 0 and l collisions with the carrier gas, respectively, T_m is the temperature of the carrier gas, and

$$\kappa = \frac{(M+m)^2}{2Mm} \tag{1.4}$$

where M and m are the masses of the target and carrier gas species, respectively [49]. To minimize κ and therefore reduce the number of collisions required to significantly cool the target species, the mass of the target species and carrier gas must be well matched. Optimal cooling is achieved for the case of $M = m$.

In the case of lithium as the target species and helium as the carrier gas as is used our this experiments, it is possible to calculate the number of collisions required to reach a reasonable temperature. Assuming $T_M = 1,000$ K, $T_m = 80$ mK, and $\kappa = (7+4)^2/(2 \times 7 \times 4) = 2.16$, on the order of twenty collisions are required to reduce the lithium temperature to below 100 mK.

Fractional entrainment of up to 1% of the supersonic carrier gas has been achieved previously, albeit with carbon atoms which are not of great interest to atomic physicists [52]. In addition, Monte-Carlo simulations of supersonic expansion suggest that fractional entrainment of up to 2-3% should be possible without significant heating of the beam [53].

Because each pulse of the Even-Lavie nozzle used in our experiments contains 10^{16} atoms, 3% of which get through the skimmer, there are 3×10^{14} carrier gas atoms past the skimmer. Assuming 3% entrainment, this gives rise to an upper limit of 9×10^{12} entrained atoms/shot before significant heating of the beam is expected.

Chapter 2

Sympathetic Cooling with Supersonic Beams

This chapter discusses the basic principles of supersonic beams which are instrumental in the experiments detailed in this thesis. In addition, some of the advantages that sympathetic cooling has over laser cooling are discussed. There is also consideration given to the advantages and disadvantages of various gases which can be used as cooling sources.

2.1 Supersonic Beams

Supersonic beams were first pioneered by physical chemists in the 20th century to produce cold gases for the purposes of spectroscopic measurements [54, 55]. Over the years these beams have been used for a variety of experiments including measurements of molecular properties such as polarizability and magnetic moments [56], precision spectroscopy [57], and measuring reaction rates [58, 59]. The expansion cools all degrees of freedom and so the

nozzles have been especially useful for molecular spectroscopy of cold organic molecules [60, 61, 62]. The reason supersonic beams are used in our experiments is their low temperatures; beams are capable of being cooled to below 100 mK through their supersonic expansion [63].

One experimental caveat of using supersonic beams is that the high gas load in the nozzle vacuum chamber necessitates a skimmer. The skimmer serves two purposes, it helps to shave off divergent particles, leaving only the coldest particles in the center of the beam, and also allows differential pumping between the nozzle chamber and the science chamber [64].

In our own experimental setup, pressure in the nozzle chamber reaches a peak value of 5×10^{-7} Torr when the nozzle is pulsed and a low pressure of 1×10^{-8} Torr after the nozzle is closed and the turbo vacuum pump removes the carrier gas which was scattered from the skimmer. If the nozzle is cooled with the cryostat then cryopumping reduces the pressure in the nozzle chamber further to 5×10^{-9} Torr. The science chamber will spike up to 5×10^{-8} Torr when the nozzle is pulsed but quickly reaches a steady state pressure of 3×10^{-9} Torr.

The resulting beam after passing through the skimmer is on the order of 100 mK. A sample image of a supersonic beam of pure helium at a nozzle backing pressure of 20 atm is shown in Fig. 2.1 at a temperature of 90 mK. This is typical of our experiment.

These low temperatures are what make supersonic beams desirable as sympathetic cooling candidates, although the do have their drawbacks. The primary drawback is the speed at which the beams move after ejection from the nozzle. Because the thermal energy of the beam is converted into translational kinetic energy, the mean velocity of the beam is fast for typical nozzle

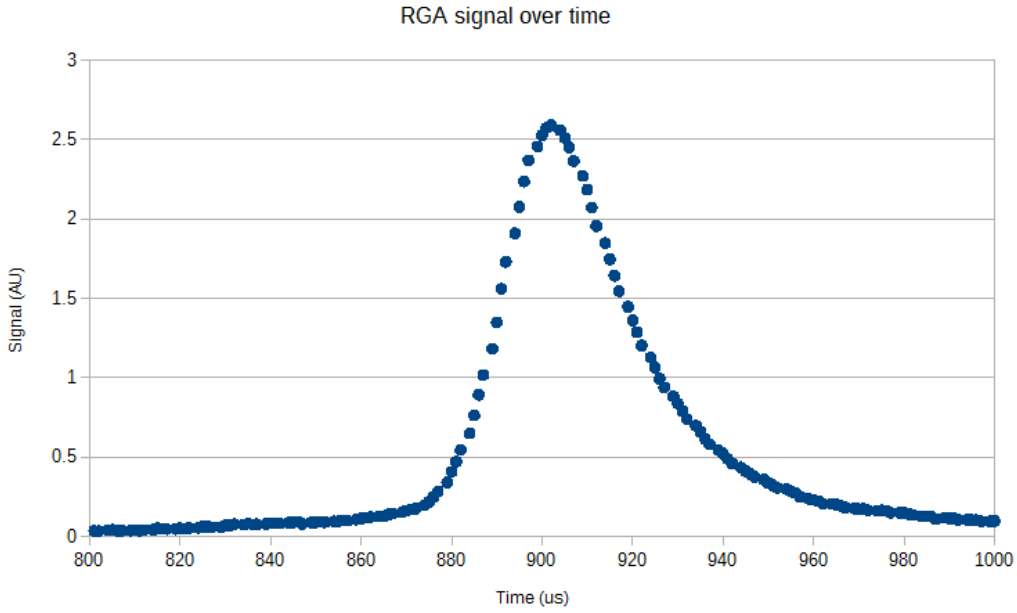

Figure 2.1: A pure helium supersonic beam with a nozzle backing pressure of 20 atm at 90 mk

Gas	T_o (K)
Helium	24
Neon	121
Argon	241
Krypton	503
Xenon	790

Table 2.1: Nozzle temperatures required by different noble gases to produce a beam travelling at 500 m/s for acceptance into the adiabatic decelerator detailed by Lavert-Ofir *et al.* [72].

temperatures. For ideal gases

$$\langle v \rangle = \sqrt{\frac{5RT_o}{N_A m}} \tag{2.1}$$

where $\langle v \rangle$ is the mean velocity of the beam, R is the ideal gas constant, T_o is the temperature of the nozzle, N_A is the Avogadro constant, and m is the mass of the particles composing the beam [65].

Although molecular beams composed of noble gases typically move at a few hundred m/s, there has been a significant push to tame them in recent years [66, 67]. By slowing the beams using a magnetic decelerator, beams can be brought to rest [68, 69, 70] and even trapped [71].

A new adiabatic slower which will serve to slow the atoms entrained in our supersonic beam is limited to an acceptance speed of 500 m/s [72]. Knowing the maximum acceptance of our slower and Eq. 2.1, it is possible to calculate the required temperature of the supersonic nozzle for different species:

$$T_o = \frac{\langle v \rangle^2 N_A m}{5R}. \tag{2.2}$$

Table 2.1 shows the nozzle temperatures required to produce a slow enough supersonic beam to be magnetically stopped using an adiabatic decelerator. It should be noted that the values of T_o included in Table 2.1 are upper bounds as the species are approximated as ideal gases for this calculation.

Clustering in the non-ideal case of a real gas can heat and increase the speed of the beam, requiring a lower nozzle temperature to produce a beam travelling at 500 m/s or less [73]. It is for this reason that only noble gases are considered in Table 2.1. Noble gases have low enthalpies of clustering and are therefore least effected by cluster formation [65]. In the specific case of helium, the gas used in this experiment, beams are atomic until the nozzle is cooled to approximately 20 K [63].

Through inspection of Table 2.1 it should be noted that only noble gas supersonic beams composed of krypton and argon do not require cooling below room temperature. By using a liquid nitrogen cryostat ($T_o = 77$ K) both neon and argon are able to be cooled enough to be accepted into the adiabatic decelerator. Helium on the other hand requires cooling to temperatures below 24 K. Cooling a nozzle in vacuum to 24 K is easily achievable through use of a commercially available 10 K cryocooler. Because of increases in recent demand, many different companies now make 10 K cryocoolers, reducing the cost to the order of $10,000 [74].

The experiments reported in this thesis were performed with a nozzle temperature of 77 K. In the future, a Sumitomo CH-210L 10 K cryocooler will be used to cool the nozzle further and slow the beam below 24 K for acceptance into the adiabatic slower.

2.2 Temperature Measurement

To properly characterize entrainment into the supersonic beam, it is necessary to be able to measure the temperature of the beam. The beam is detected using a residual gas analyzer (RGA) operated in a time of flight mode for characterization. As helium strikes the hot filament on the RGA it is ionized and pulled toward the detector through a quadrupole mass analyzer. By setting the radio frequency on the mass filter to eject particles that do not have a mass to charge ratio of 4 amu/C, only helium is detected.

By fitting a Gaussian to the data acquired by the RGA and taking the full width at half maximum (FWHM), it is possible to determine the speed ratio of the beam

$$S = \frac{t_o\sqrt{\ln 2}}{FWHM} \tag{2.3}$$

where S is the speed ratio of the beam, t_o is the time between opening the nozzle and the center of the Gaussian recorded by the RGA, and the FWHM is the full width at half maximum of the fitted Gaussian [62].

The speed ratio is simply the ratio of the mean forward velocity of the beam divided by the mean transverse velocity of the beam. The higher the speed ratio the more directional the beam is and therefore the colder it is; because of this, a molecular beam with a large speed ratio is desirable.

Taking the speed ratio, it is possible to calculate the temperature of the beam

$$T = \frac{T_o}{1 + 2/5S^2} \tag{2.4}$$

where T is the temperature of the beam and T_o is the temperature of the nozzle. Knowing the temperature of the beam is important for understanding

the impact of entrainment. For example, it may be optimal to entrain fewer atoms while lowering the temperature of the beam as optimal entrainment is defined by optimized phase-space density.

Phase-space density is defined as

$$\rho = n\lambda^3 \tag{2.5}$$

where n is the atomic density and λ is the de Broglie wavelength of entrained particles [75]. Because

$$\lambda = \frac{\hbar\sqrt{2\pi}}{\sqrt{Mk_BT}} \tag{2.6}$$

where M and T are the mass and temperature of the entrained atoms,

$$\rho \propto \frac{n}{T^{3/2}} \tag{2.7}$$

meaning that both temperature and atomic density play a critical role in determining the phase-space density. Because of the dependence of phase-space density on both temperature and atomic density it is important to not neglect the temperature of the beam.

Simply entraining more atoms into a beam is not optimal as supersonic beams have a limited cooling capacity and eventually the temperature will start to rise, leading to a decrease in phase-space density. This decrease is further exacerbated by the fact that phase-space density is inversely proportional to the square root of temperature cubed while only being directly proportional to the atomic density.

It is because of the importance of temperature in our experiments that we have chosen to use an Even-Lavie valve. Even-Lavie nozzles have trumpet

shaped openings which produce a more directional beam than the traditional conical designs, leading to lower beam temperatures [73, 76]. In addition, Even-Lavie valves provide a much denser expansion of gas allowing for higher density of entrained particles given the same entrainment fraction [77].

Chapter 3

Methods of Entrainment

This chapter considers a variety of methods which can be used to entrain particles into a supersonic beam. Because the majority of atoms which are of interest to atomic physicists are in the solid state at room temperature, vaporization is required for most gas phase experiments. There are a number of ways to generate these atomic sources, some of which are described in detail below.

3.1 Entrainment Considerations

One consideration for generating atomic sources is that it is useful to match the atomic and cooling sources. As previously discussed, our experiment utilizes a pulsed nozzle which emits a supersonic beam with which to sympathetically cool the vaporized atoms. Because only a portion of the beam will travel through the skimmer and because the nozzle is operated in a pulsed rather than continuous mode, it is necessary to consider both spatial and temporal factors.

To match the atomic source spatially the source should only eject atoms into the path of the beam or return atoms which are not entrained into the beam to the source. To match the atomic source with a pulsed nozzle temporally the source should only eject atoms at the time of the pulse or return atoms which are not entrained into the beam to the source. An atomic source which emits atoms only when the nozzle is pulsed is well matched temporally while a source that only emits atoms in the trajectory of the supersonic beam is well matched spatially.

As discussed in Sec. 1.2.2, there are other considerations inherent to sympathetic cooling which are also important to consider with respect to an entrainment source. For example, it is important to match the masses of the carrier gas and target species as this reduces the number of collisions necessary to cool the target particles [78, 79].

Fortunately, lithium and helium which are the target species and carrier gas used in these experiments have similar mass with $\kappa = 2.16$, and helium creates a colder supersonic beam than other gases which allow the target species to reach extremely cold temperatures. It is also important to have a low ratio of inelastic collisions to elastic collisions as inelastic collisions are disruptive to the cooling process [47, 49].

3.2 Experimental Setup and Detection

Our experimental setup is primarily enclosed in two large 8 inch ConFlat (CF) crosses separated by a 5 mm diameter skimmer. They are held at approximately 1×10^{-8} Torr for the nozzle chamber (shown on the left in Fig. 3.1) and 3×10^{-9} Torr for the science chamber (shown on the right in Fig. 3.1).

These two chambers are connected by a 2 3/4 inch CF cross which is used for spectroscopy detection as well as a 2 3/4 CF bellows and are differentially pumped by two 8 inch Varian Turbo-V 550 L/s turbo pumps. In addition to being pumped by one 8 inch Varian Turbo-V 550 L/s turbo pump, the nozzle chamber is also cryopumped by a 77 K cryostat during experiments. When the nozzle is not being pulsed and the nitrogen cryostat is filled the pressure can reach as low as 5×10^{-9} Torr.

The nozzle chamber houses the Even-Lavie valve as well as the entrainment tools (with the exception of the heat pipe which is placed between the nozzle and science chamber) while the science chamber houses the wire detector and will eventually house a magnetic trap for the slowed particles. The final chamber on the right which is used for RGA detection of the supersonic beam is held at approximately 1×10^{-9} Torr and is pumped by a 4 1/2 inch Varian Turbo-V 70 L/s turbo pump. This chamber is separated from the science chamber by a solid copper CF gasket which has a 2 cm hole bored through the center.

Because the number of entrained atoms in a supersonic beam is less than the number of carrier gas atoms in a beam by a factor of 100 or more, it is difficult to detect entrained atoms using a RGA. Because of this, a new method of detection is required. Measurements reported in this chapter were taken with a Langmuir-Taylor detector [80, 81]. The Langmuir-Taylor detector used in these experiments is based on the design of Delhuille *et al.* [82] and is shown in Fig. 3.2.

When a lithium atoms strikes the rhenium wire in the center of the

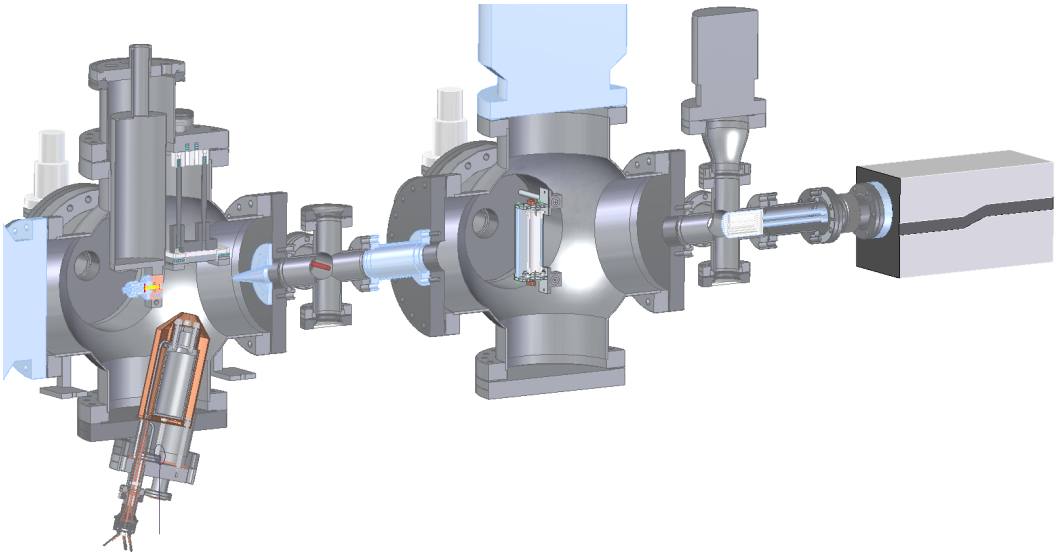

Figure 3.1: Solid Edge drawing of the complete experimental setup with pulsed ribbon and directional oven displayed. On the left side of the image is the nozzle chamber housing a 77 K cryostat with an Even-Lavie valve mounted underneath. Both the directional oven and ribbon are shown between the nozzle and skimmer. To the right of the skimmer is a red spectroscopy laser followed by a wire detector and RGA. Total distance separating the nozzle from the white ionizer connected to the RGA is 89 cm.

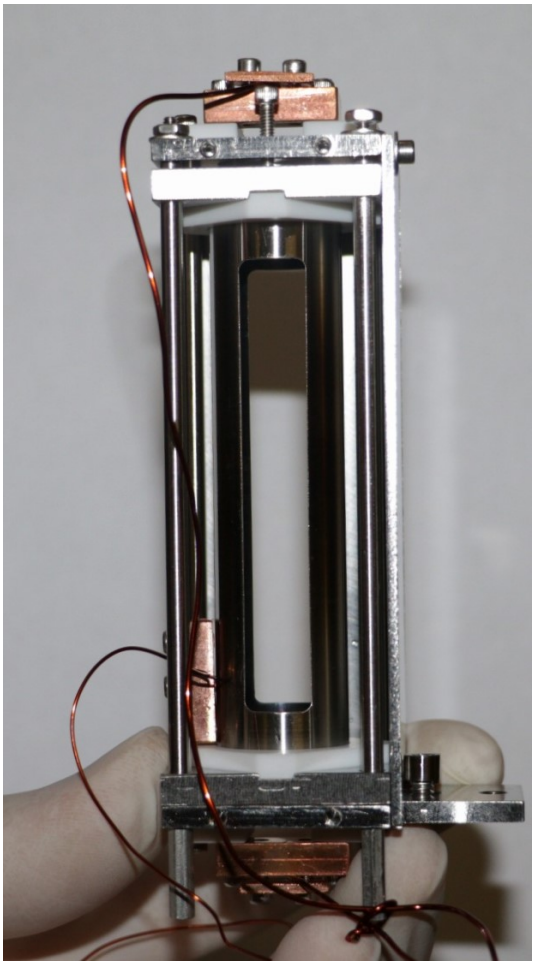

Figure 3.2: Langmuir-Taylor detector used to detect lithium entrainment in our experiment. The detector is shown here without a heated wire in the center of the structure as this picture was taken while maintenance was being performed.

detector it is ionized with probability

$$P_+ = \frac{1}{1 + (g_o/g_+)exp[(I - \Theta)/k_B T]} \tag{3.1}$$

where g_o and g_+ are the statistical weights of ion and atom ground states (in the case of alkali atoms such as lithium $g_o/g_+ = 2$), Θ is the work function of the rhenium wire, I is the ionization potential of the atom, k_B is the Boltzmann constant, and T is the temperature of the rhenium wire [82]. For typical operation in our experiment, a lithium atom is ionized with $P_+ \approx 0.3$.

If the rhenium wire is held at room temperature then the ionized particle will stick to the detector and will not be detected. However, by running a current of roughly 3–4 A through the wire in the center of the detector, the wire reaches a temperature of approximately 2,000 K. At this temperature alkali ions do not stick to the detector, but instead are pulled toward the negatively biased structure surrounding the wire. By monitoring the ion current, it is possible to detect the number of atoms which strike the wire as a function of time.

The data displayed in Fig. 3.3 was acquired by positioning the Langmuir-Taylor detector at a known position in space using a linear manipulator and monitoring the ion current from ionized lithium atoms over time. By integrating the signal over time the total number of entrained atoms at this point in space is known since the wire has a known width. By translating the wire across the beam and integrating over time again another data point is acquired. By performing this over the entire width of the beam and integrating these points it is possible to determine the total number of entrained atoms in the beam. At 60 cm away from the nozzle source where our detector is located

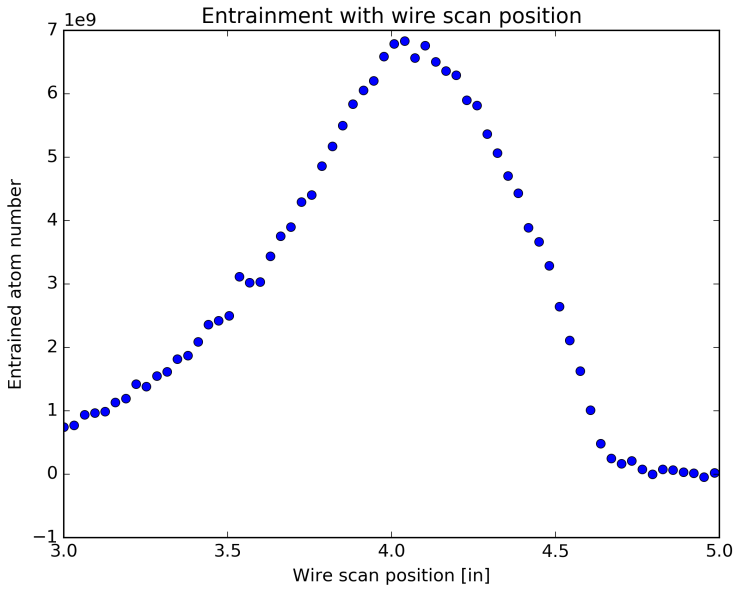

Figure 3.3: Langmuir-Taylor detector signal with 2×10^{11} atoms. Data was taken using both the pulsed ribbon and directional oven operated at 825 K at a repetition rate of 1 Hz.

a 100 mK beam is approximately 4 cm wide.

Fluorescence and absorption measurements are also useful in determining the number of entrained atoms in a supersonic beam. An unfortunate drawback of using a Langmuir-Taylor detector is that the detector itself is destructive to the supersonic beam.

Because the wire used to ionize the entrained atoms disrupts the beam, the RGA detects an artificially heated carrier gas. The primary advantage of using fluorescence and absorption measurements is that entrained particles can be observed in parallel with supersonic beams while a Langmuir-Taylor detector limits experimentalists to serial measurements of entrained atom number and beam temperatures.

3.3 Laser Ablation

Laser ablation has been used for the purpose of vaporization with great success for many years [49]. By using a pulsed laser, a large amount of energy is transferred to the absorbing medium over a short period of time. Because of the high concentration of energy, there is local vaporization in the area immediately surrounding the laser pulse [83, 84]. By timing the laser ablation pulse with the supersonic nozzle pulse, it is possible to entrain the ablated media into the resulting supersonic beam, which will cool the ablated material and accelerate it in the forward trajectory of the beam [85].

Laser ablation has been used in many supersonic beam experiments as a source for entrainment over the past 20 years, and has achieved considerable success including loading molecules into ions traps [85], as a source for inductively coupled plasma mass spectrometry [86] and for precision spectroscopy experiments [87]. However, these experiments do not require a large number of entrained atoms.

In order to improve on the limited cold atom flux provided by laser cooling, it is necessary to entrain a large number of atoms into the supersonic beam. Our experiment used a Minilite 1064 nm Nd:YAG ablation laser with a pulse energy of 50 mJ and pulse width of 5 ns fired at a target shown in Fig. 3.4. A Solid Edge rendering of the target in vacuum with the nozzle and skimmer is shown in Fig. 3.5.

Although we were able to efficiently generate a high density cloud of lithium atoms, these single atoms quickly condensed into clusters in the expanding plume [88, 89]. The formation of these clusters compromised the cooling ability and therefore the entrainment efficiency of the beam for two

Figure 3.4: Ablation target taken out of vacuum. While in vacuum the target is composed of highly purified lithium although after removal from vacuum the target degrades over time and forms a white oxide layer as shown here.

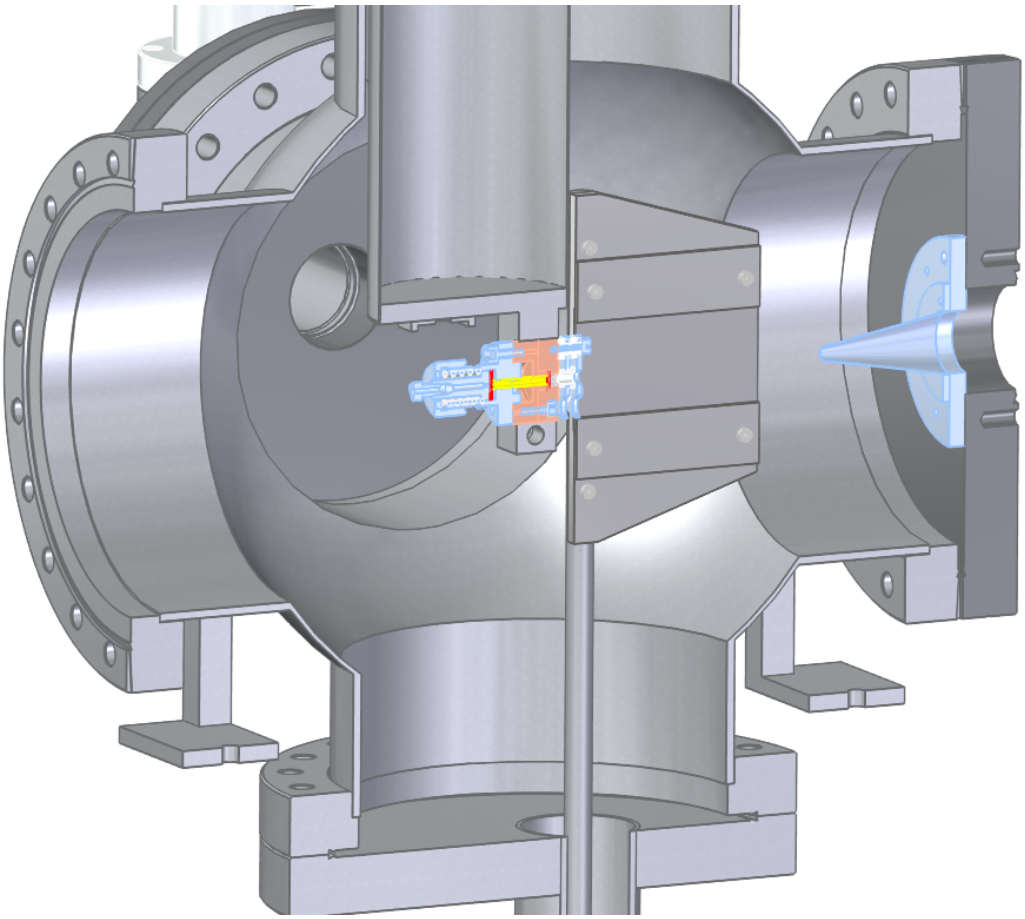

Figure 3.5: Solid Edge rendering of the ablation target used for entrainment. The ablation target is placed between the nozzle and skimmer and the laser was fired in time with the nozzle to achieve optimal entrainment.

reasons.

The first is that supersonic beams are most efficient at cooling similar mass species [62, 79], which is one of the reasons why helium was chosen as the carrier gas for lithium entrainment. Since the clusters are composed of grouping of 10–1,000 atoms, the mass ratio between the carrier gas and the clusters becomes large, thereby decreasing the ability of the carrier gas to efficiently cool the target species and resulting clusters.

The second reason is that there are more energetic particles being entrained into the supersonic beam given a set number of single atoms. Since the supersonic expansion is composed of a limited number of atoms, the beam has a limited cooling capacity. Because the clusters themselves are composed of many single atoms, one cluster can eat away as much cooling power as 1,000 single atoms while contributing nothing to cold atom flux [88, 90].

Laser ablation is a messy method of entrainment because of the clusters which are also entrained into the beam. If laser ablation resulted in a pure atomic cloud which was entrained into the supersonic beam then the method would likely yield better results. However, cluster formation is inevitable if the result of laser ablation is to yield a large number of atoms.

The limits of laser ablation as a method of entrainment found in this thesis were 2×10^{10} entrained atoms per shot at a beam temperature of 750 mK.

3.4 Effusive Oven

Because entrainment of atoms using the laser ablation technique lead to significant heating of the supersonic beam a new atomic source was required. An

oven was developed to test entrainment in a different manner. The advantage of using an oven as a source of atoms is that there is no clustering. The cause of clustering in ablation plumes is the extremely high local density of ejected particles due to rapid heating and the correspondingly rapid cooling [83, 88, 90].

In contrast, an oven emits atoms over a relatively large area (in the case of our effusive oven, 28 mm^2). By spreading the energy used to heat the sample out, a number of ejected particles comparable to laser ablation can be generated but without the high density which results in clustering. This purely atomic source is much less perturbative than ablation and has a negligible effect on the temperature of the beam.

Unfortunately, the oven which is shown in Fig. 3.6 and in Fig. 3.7 with the nozzle and skimmer was only designed to operate at temperatures below 875 K. Due to short heating wire lengths used to heat the nozzle of the oven, temperatures in excess of 875 K led to heating wire failure. However, a temperature this high is still enough to give rise to a local lithium vapor pressure of 50 mTorr [91, 92].

Ultimately, the effusive oven was limited to 4×10^{10} atoms entrained per shot at an oven temperature of 875 K, however there was no noticeable heating of the beam which is in stark contrast to laser ablation. The temperature of both the pure helium beam and the helium beam with 4×10^{10} lithium atoms entrained was 100 mK.

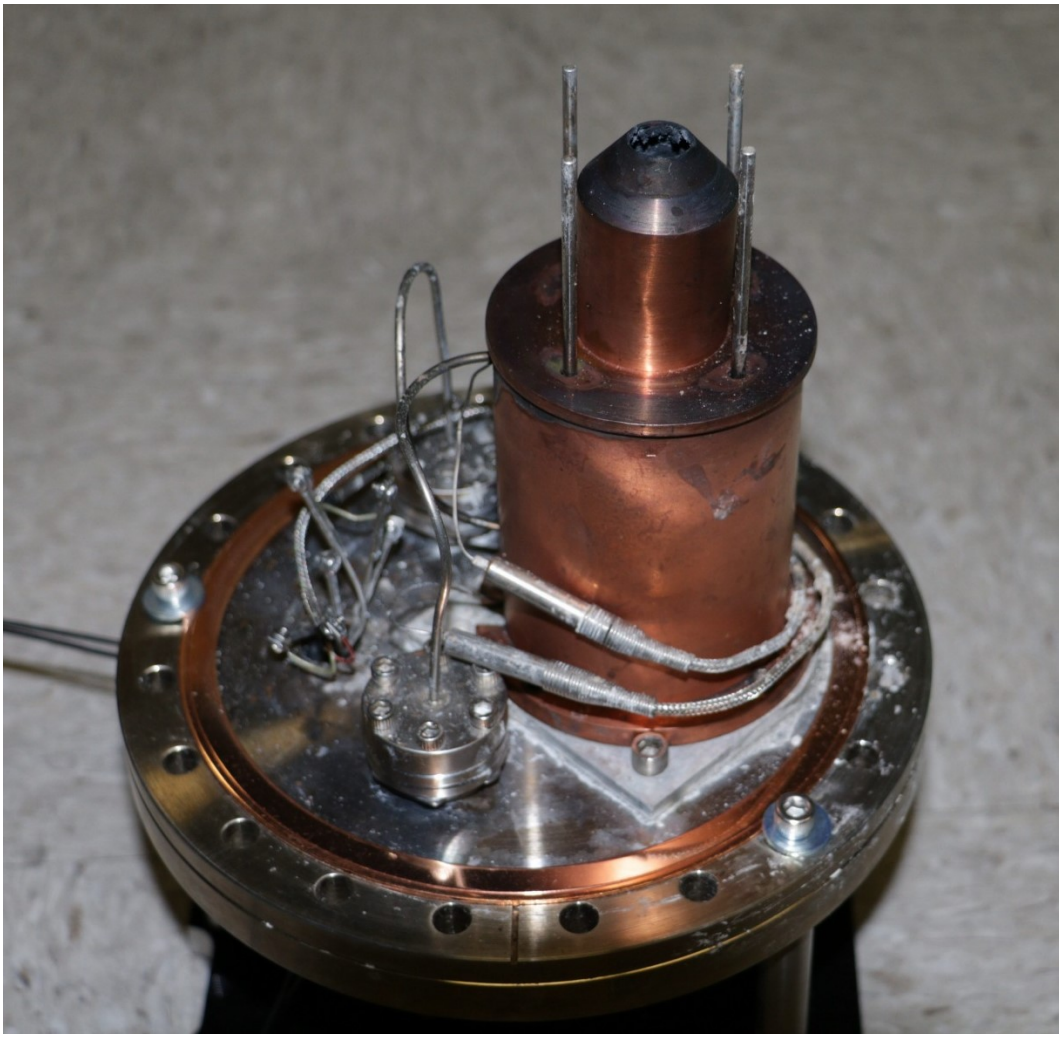

Figure 3.6: Effusive oven after being taken taken out of vacuum.

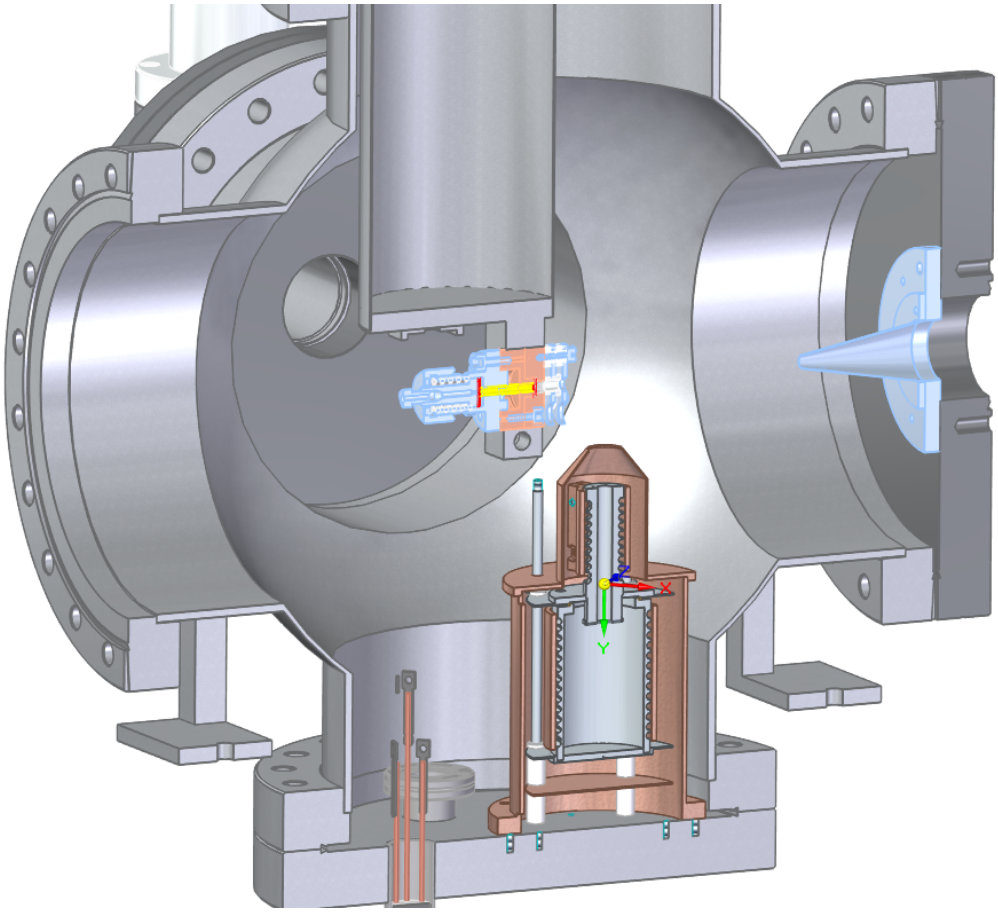

Figure 3.7: Solid Edge rendering of the effusive oven between the nozzle and skimmer.

3.5 Directional Oven

Even though entrainment using the effusive oven at 875 K was successful, there were experimental hindrances which caused rethinking of the design. Namely, only one or two experiments were able to be performed before the oven had to be refilled due to depleted lithium.

There are two main considerations which are able to be optimized with respect to the entrainment source: pulsing the atomic source and aiming the source toward the path of the beam to avoid wasting atoms. Although it is difficult to create an oven with a low enough thermal mass to generate vapor in pulses [93], it is relatively easy to control the oven in space by limiting the divergence of the beam [94]. By designing a directional oven as shown in Fig. 3.8, we are able to optimize spatial parameters although temporal parameters are still not optimized.

The directional oven works by limiting the number of divergent particles leaving the oven. This limitation is achieved by placing capillaries shown in Fig. 3.9 at the exit point of the oven which allow particles travelling toward the path of the supersonic beam to exit, while hindering particles which would be outside the path of the beam. The idea of limiting the flux of divergent particles is not new, and was instrumental in the construction of the first maser [95], but had not been applied to atomic physics experiments where the atoms of interest required significant heating until recently.

By heating both the reservoir to generate a hot vapor of lithium atoms and the capillaries which control the directionality of lithium atoms, Senaratne *et al.* [96] was able to apply this technique to alkali atoms commonly used in atomic physics experiments. When divergent atoms collide with the wall of

Figure 3.8: Directional oven taken out of vacuum. The two wires shown heat the reservoir and capillaries.

Figure 3.9: Close up of capillaries used to limit the divergence of the directional oven.

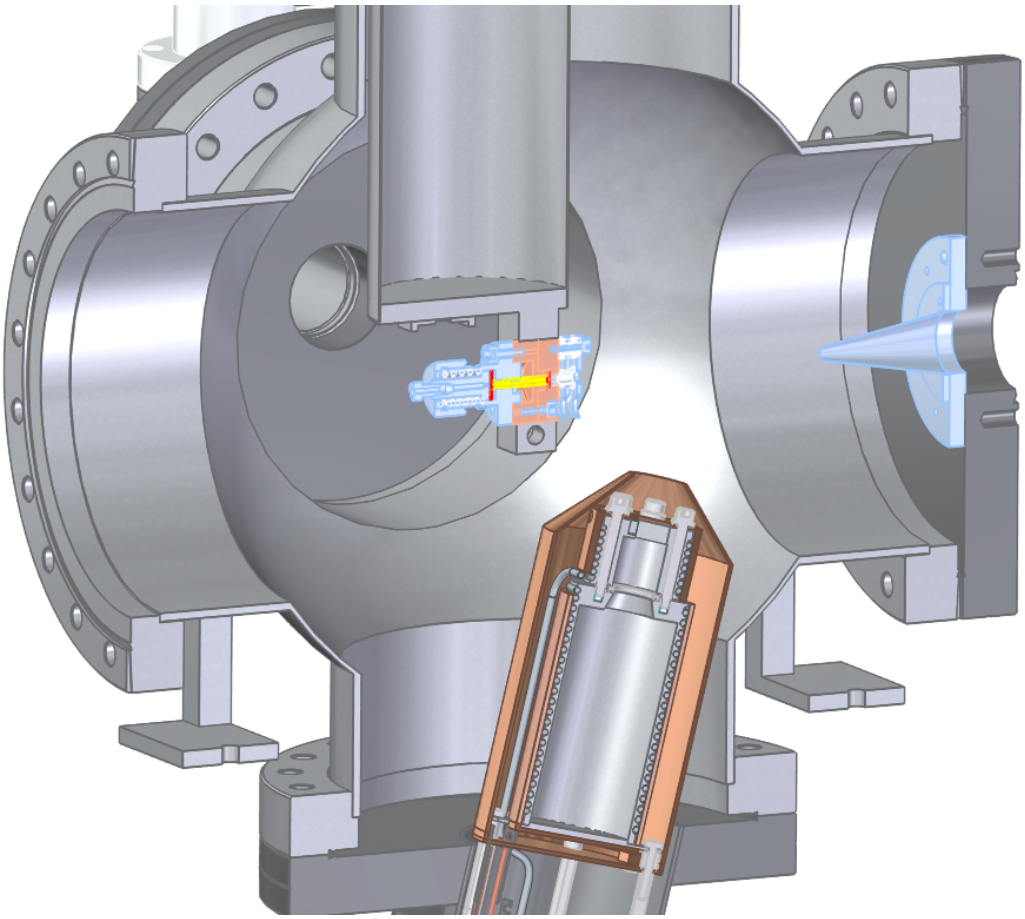

Figure 3.10: Solid Edge rendering of capillary oven.

a capillary they are adsorbed and subsequently re-emitted. In this process there is no memory of a previous trajectory before striking the wall since the rescattering process is equally likely to eject an atom at any angle over 2π. The result is that the majority of divergent atoms are returned to the reservoir, limiting wasted material.

One limitation of the directional oven shown in our experiment in Fig. 3.10 is that divergent atoms are returned to the reservoir if they only interact with the capillary walls. While this is a good approximation at low reser-

voir temperatures, higher temperatures result in a greater pressure within the capillaries themselves, leading to atom-atom collisions. Because there is a net flux through the capillaries as well as a significant number of collisions between atoms at high reservoir temperatures, the directional oven eventually loses its directionality.

The directional oven at 875 K was ultimately limited to 4×10^{10} atoms entrained per shot at a beam temperature of 100 mK. Although this number is identical to the effusive oven, the main advantage is a longer oven life. By limiting the number of wasted atoms, the experiment stays operational for longer.

It is important to remember that only atoms which would have missed the supersonic beam of helium are restricted from leaving the directional oven. Because of this, it is not surprising that there is no increase in efficiency from the directional oven over the effusive oven when operated at the same temperature.

3.6 Pulsed Ribbon

The directional oven conserved many atoms that would have been wasted at low reservoir temperatures, but when the temperature of the reservoir was pushed high enough the beam eventually became more divergent. Because of this, at the temperatures required to entrain 4×10^{10} atoms/shot, the directional oven wasted a significant number of atoms which severely limited the length of time that the oven could be operated before depletion.

To fix this problem, a thin (50 μm) Nichrome ribbon shown in Fig. 3.11 was installed above the directional oven that was able to be flash heated with

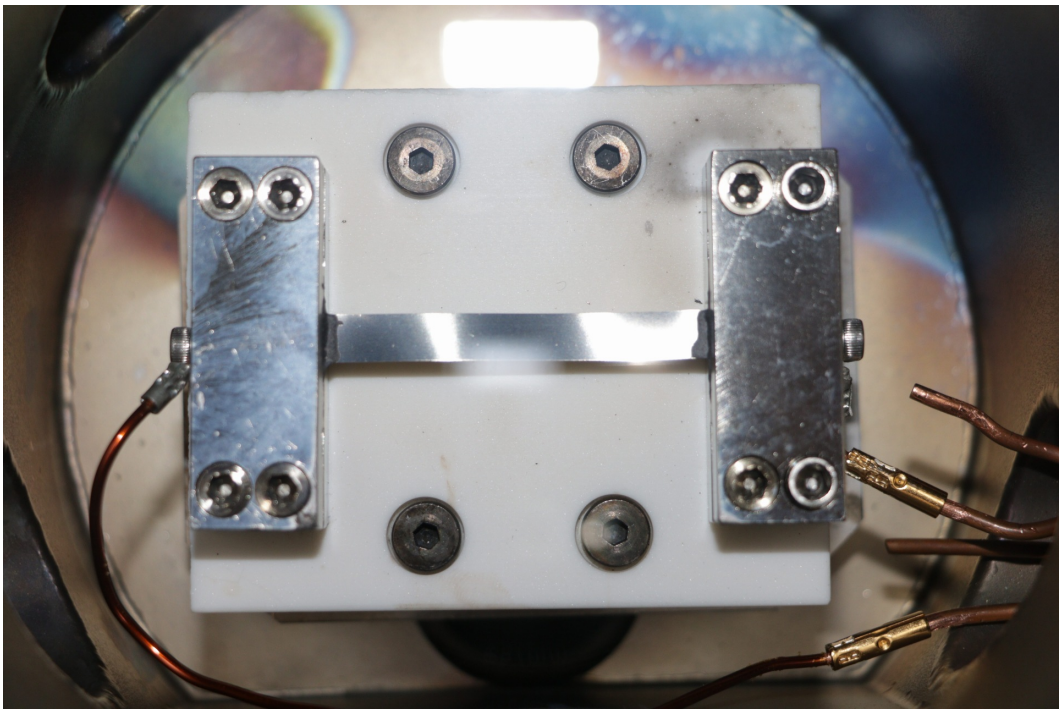

Figure 3.11: Ribbon made of Nichrome shown from the bottom of the nozzle chamber. The ribbon is flash heated using an IGBT which controls a 150 mF capacitor bank charged to 300 V. The directional oven is aimed at the ribbon and the supersonic beam shoots from the left side of the figure to the right.

a high current pulse. The directional oven is kept at a low enough temperature to maintain its directionality (825 K) and aimed at the ribbon which measured 6 mm wide and 50 mm long, providing a constant flux of lithium for coating. In time with the supersonic beam, a high current pulse resistively heated the ribbon, causing the adsorbed lithium to be ejected into the path of the beam. In this manner, we were able to optimize temporal aspects of entrainment as well as spatial aspects by combining the ribbon with the directional oven. The ribbon as used in tandem with with the directional oven is shown in Fig. 3.12 and 3.13.

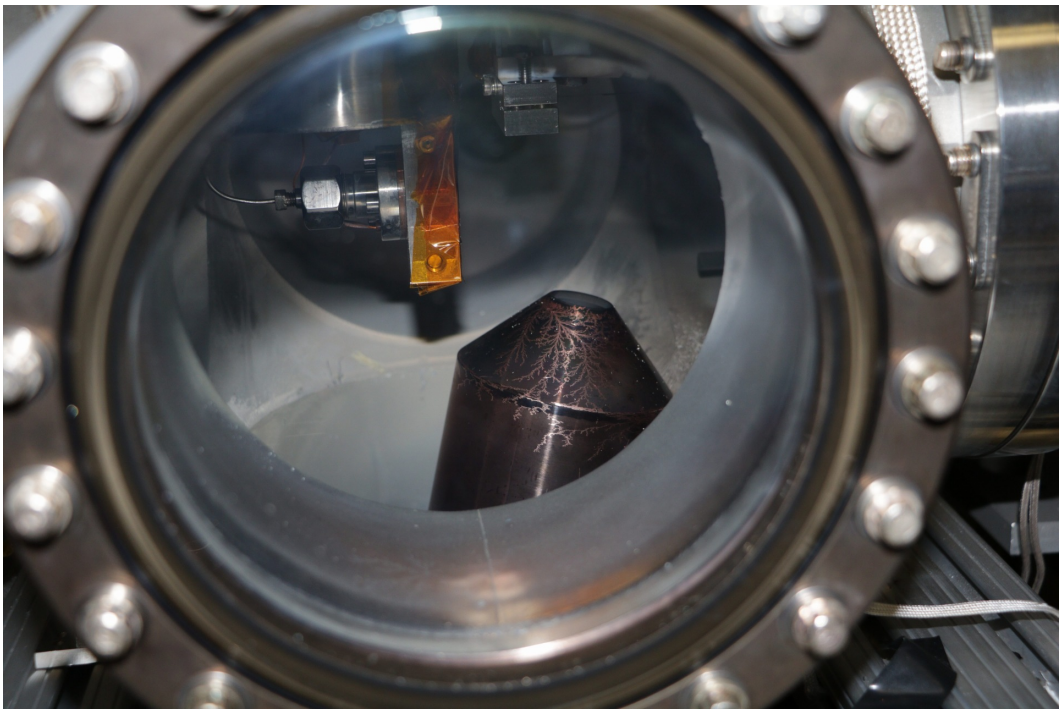

Figure 3.12: Experimental setup of ribbon and directional oven with the nozzle shown on the left.

It is because the ribbon is so thin and the thermal mass so low that we are able to efficiently heat the ribbon in sync with the nozzle. Because the surface area of the ribbon is large relative to its volume, the temperature decays primarily through radiation at an extremely fast rate, on the order of tens of milliseconds [97].

The ribbon design is somewhat similar to the ovens used by DeVoe and Kurtsiefer [98] and Vittorini, Wright, Brown, Harter, and Doret [99], but instead of placing the ribbon inside of a blackbody shield, the ribbon is exposed and the supersonic beam travels between the two oven stages.

The limits of entrainment using both a directional oven at 825 K and a flash heated ribbon in tandem are 2×10^{11} atoms entrained per shot at a

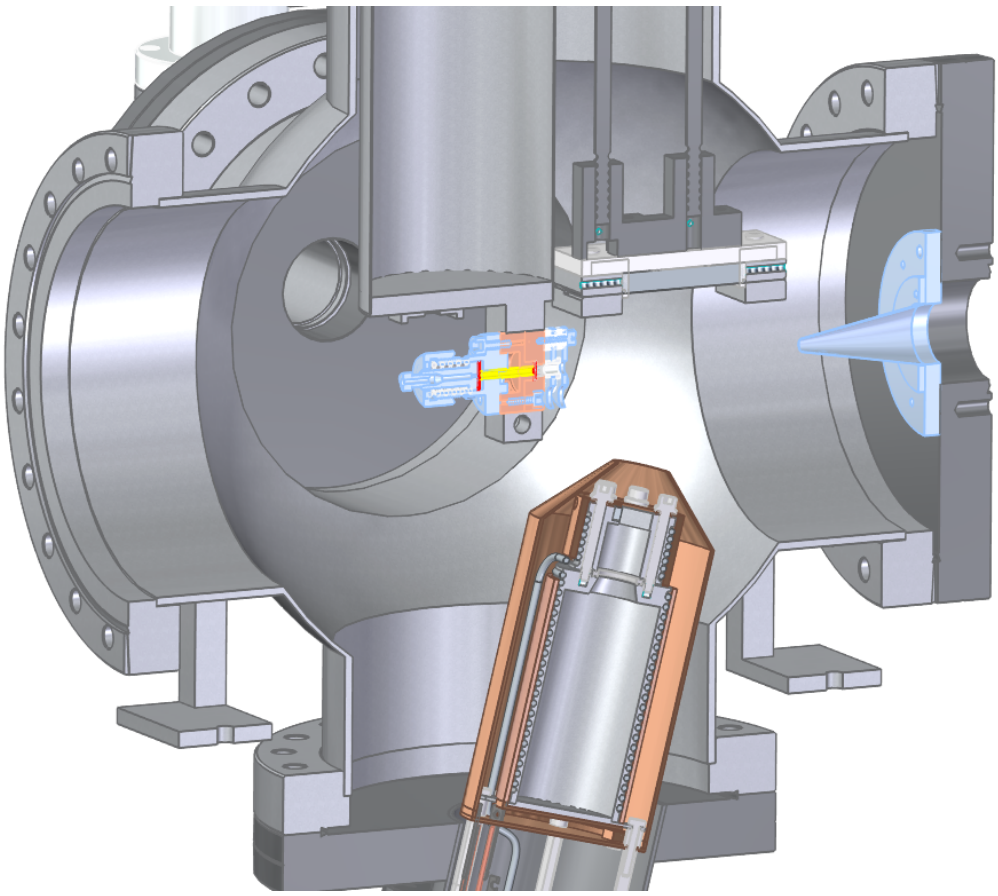

Figure 3.13: Solid Edge rendering of the ribbon and directional oven placed between the nozzle and skimmer.

beam temperature of 100 mK at a repetition rate of 1 Hz. For comparison, the directional oven entrains 1×10^{10} atoms entrained per shot at a temperature of 825 K. Using the ribbon in tandem with the directional oven amplifies the signal to 2×10^{11}, yielding a $\times 20$ amplification factor.

3.7 Heat Pipe

The final entrainment design discussed in this thesis is a heat pipe. The heat pipe is similar in concept to a reflux oven where atoms which strike the side of an oven and therefore would not have been of use in an experiment are returned to the main reservoir [100]. The design used in this experiment resembles the charge transfer cell used by Boffard *et al.* [101]. As can be seen in Fig. 3.14 and 3.15, the supersonic beam shoots through the pipe itself while lithium atoms enter the pipe from below.

The heat pipe relies on the concept of capillary action and surrounding the pipe with a medium through which the atoms ejected from the oven can be wicked back to the reservoir [102]. This is accomplished by cutting a fine mesh (316 stainless steel, 35 μm wire diameter with 70 μm opening) and wrapping the mesh around the inside of the pipe while letting strands of the mesh dangle into the reservoir.

By maintaining the temperature of the heat pipe slightly above the melting point of the atoms being ejected from the hot oven the ejected atoms will condense on the mesh and be wicked toward the hottest region of the pipe, the reservoir [103]. This is achieved by only heating the reservoir while letting the rest of the pipe be heated by thermal conduction [97].

Because of the low temperature of the pipe relative to the temperature

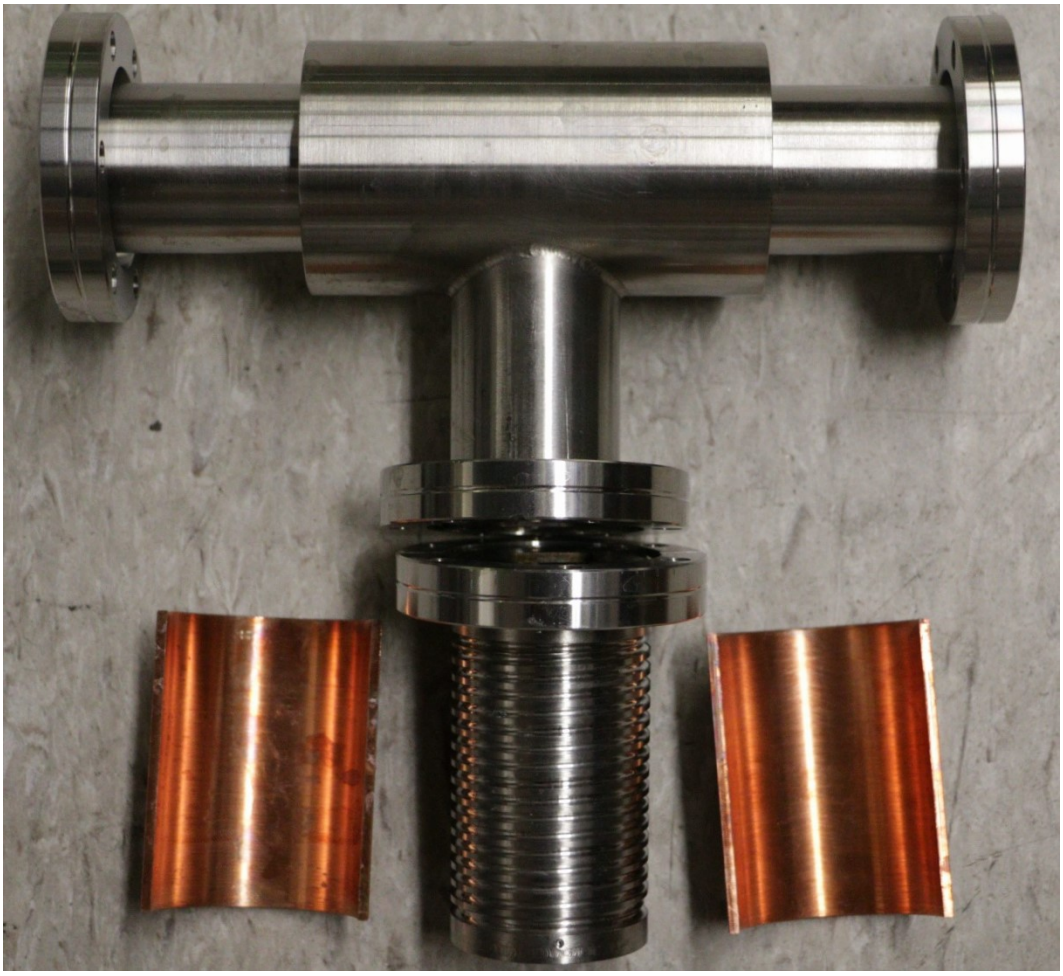

Figure 3.14: Heat pipe shown disassembled and detached from the experiment.

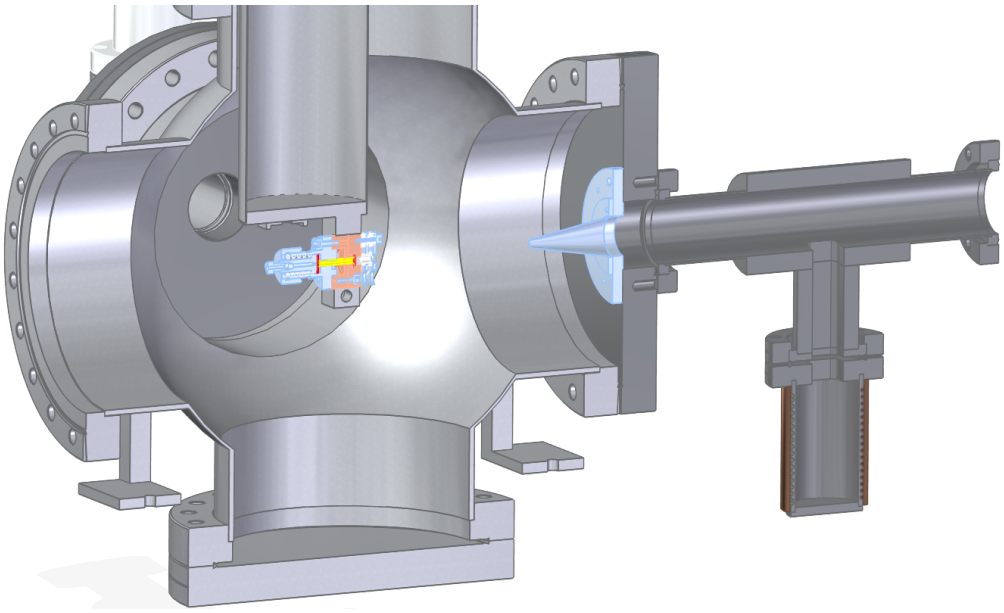

Figure 3.15: Solid Edge rendering of heat pipe placed after the skimmer.

of the reservoir, the majority of pressure inside the pipe is from the reservoir which does not have a direct line of sight out of the pipe. This limits the number of non-entrained atoms which are able to leave the pipe.

Fig. 3.16 and 3.17 show the temperature gradients simulated in COMSOL for a reservoir held at 800 K after 60 minutes. The center region of the pipe is in a temperature range where lithium is a liquid while the outer flanges are below the melting point of lithium. This gradient allows lithium to flow back toward the reservoir while holding the pipe itself at a temperature low enough to not have a significant vapor pressure [91, 92].

Although the heat pipe has not been used for purposes of entrainment yet, preliminary tests have been performed which confirm a significant vapor pressure within the pipe, but a drastic reduction outside the pipe. A cold cathode gauge located close to the heat pipe reported an observed pressure of

7×10^{-5} Torr while the heat pipe was at a temperature of 1,000 K. At these temperatures, lithium has a vapor pressure of 7×10^{-1} Torr [91, 92] leading to a pressure suppression factor of 10,000.

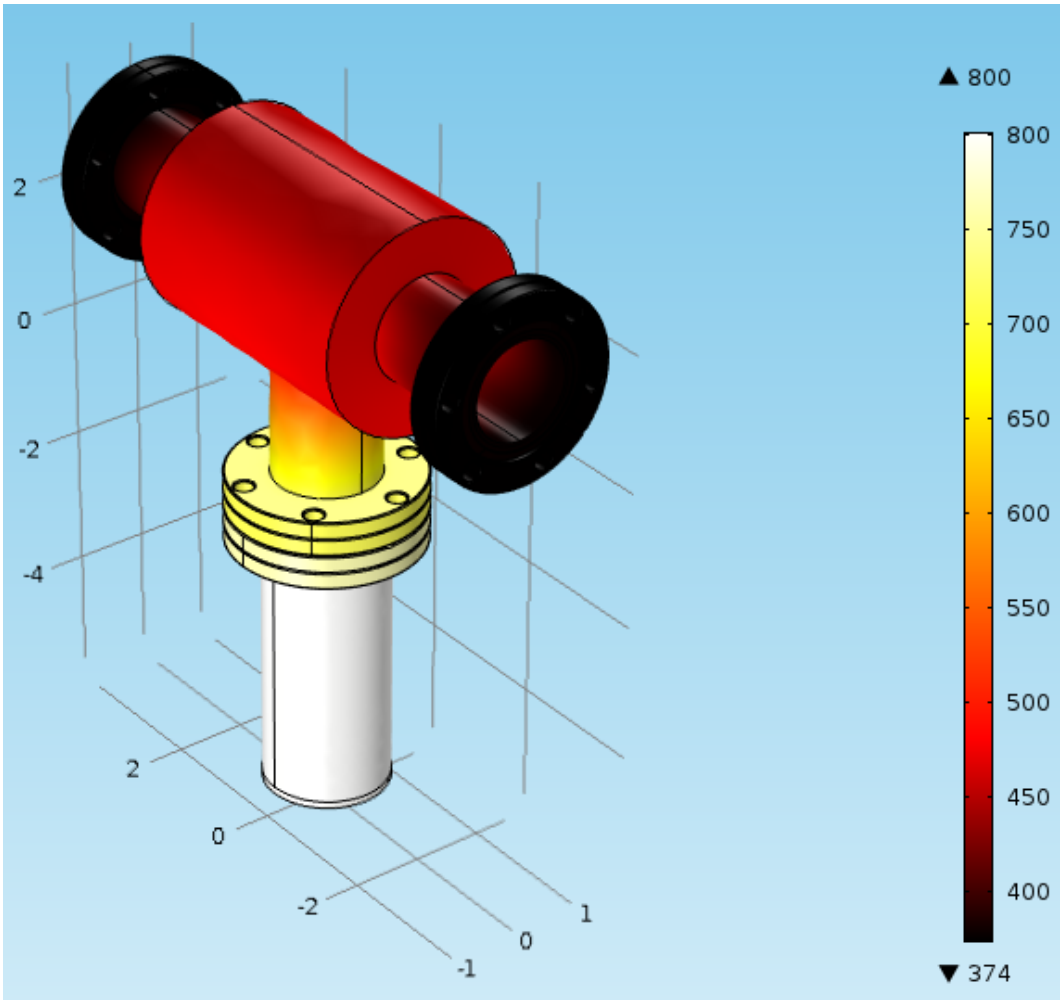

Figure 3.16: Finite element simulation of the heat pipe using COMSOL. The reservoir temperature was set to 800 K and the rest of the heat pipe was allowed to heat up over 60 minutes.

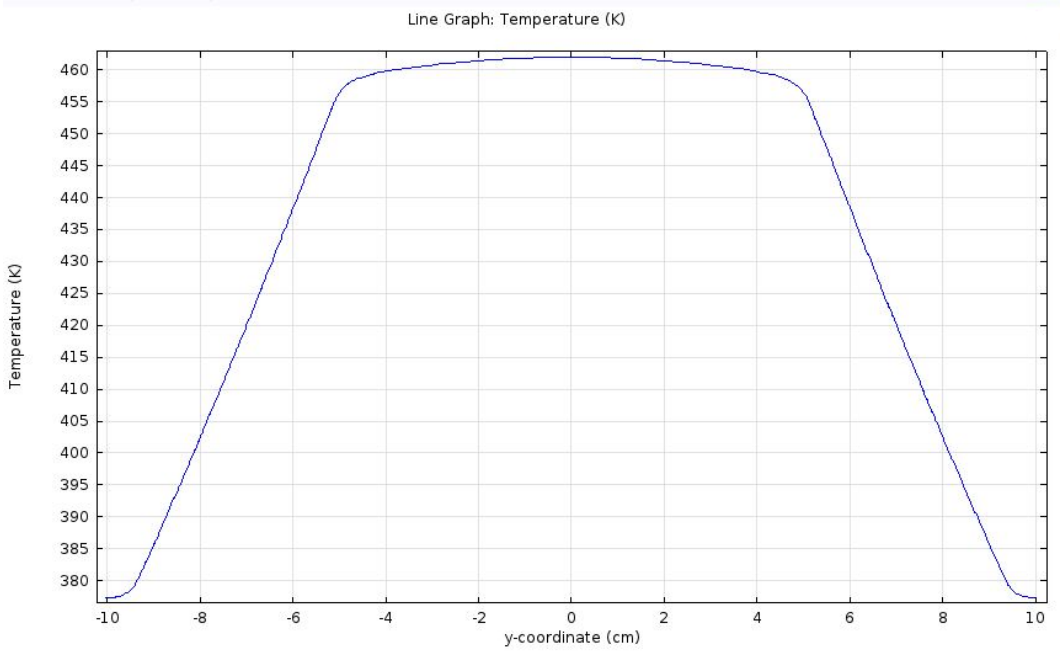

Figure 3.17: Temperature profile of the heat pipe shown in Fig. 3.16. The y-coordinate runs along the topside interior of the heat pipe with its axis in line with the supersonic beam. The increased gradient exhibited at -5 and 5 cm is the end of the thermally conductive pipe and the beginning of thin vacuum walls which serve to thermally isolate the pipe from the nozzle and science chambers.

Chapter 4

Conclusion

Research on cold atoms is a popular and versatile area, filled with experiments ranging from using strontium clocks to physically realize the meter and second [104], to using interferometry with cesium atoms to put constraints on dark energy [105], to using spectroscopy on dysprosium to search for dark matter [106]. The entrainment techniques discussed in this thesis are only the first step in a new cooling process which will enhance and expand the possibilities of this field.

It has been shown that by using a pulsed ribbon which is constantly doped by a directional oven, up to 2×10^{11} atoms can be entrained into a supersonic beam in a single shot at a repetition rate of 1 Hz yielding a cold atom flux of 2×10^{11} atoms/s. By combining this entrainment method with an adiabatic coilgun [72], atom number is able to be conserved while bringing the particles to rest and trapping them in a magnetic trap.

In comparison, laser cooling saturates at a cold atom flux of 10^9 atoms/s [14]. By pairing entrainment with a pulsed ribbon and directional oven with an adiabatic decelerator capable of slowing atoms at a repetition rate of 1 Hz

Method of Entrainment	Entrainment Efficiency (atoms/shot)	Temperature (mK)
Laser Ablation	2×10^{10}	750
Effusive Oven	4×10^{10} (875 K)	100
Directional Oven	4×10^{10} (875 K) 1×10^{10} (825 K)	100
Pulsed Ribbon	2×10^{11} (825 K)	100
Heat Pipe	No data yet	No data yet

Table 4.1: Comparison of entrainment efficiency of the different entrainment techniques outlined in this thesis and the resulting beam temperatures. The pulsed ribbon experiment was achieved through constant doping of the ribbon using the directional oven held at 825 K.

which is the current limit of the decelerator desceribed by Lavert-Ofir *et al.* [72], our new method of cooling will have a higher cold atom flux than laser cooling by a factor of 200.

The limits of the various entrainment techniques described in this thesis are shown in Table 4.1 which shows optimal entrainment being reached by a pulsed ribbon used in tandem with a directional oven. However, the pulsed ribbon starts to lose effectiveness when it is pulsed at a repetition rate faster than 1 Hz which is why the heat pipe was designed and optimized for experiments operating at faster repetition rates. The advantages and disadvantages of each entrainment method are outlined in Table 4.2.

Method of Entrainment	Positives	Negatives
Laser Ablation	Easy to implement	Significant beam heating
Effusive Oven	Easy to implement	Wastes the majority of atoms
Directional Oven	Limits wasted atoms	Works best when supplemented with pulsed ribbon
Pulsed Ribbon	Large entrainment numbers for low repetition rates (< 1 Hz)	Loses effectiveness at higher repetition rates (> 1 Hz)
Heat Pipe	Arbitrarily high repetition rate	Unproven

Table 4.2: Advantages and disadvantages of each entrainment technique described in this thesis.

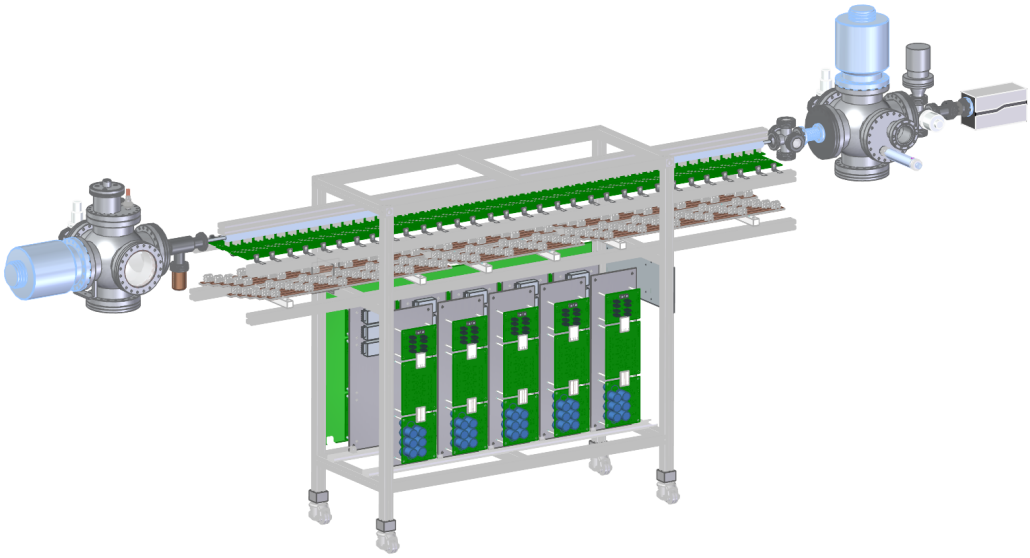

Figure 4.1: Solid Edge rendering of the experimental setup complete with heat pipe and adiabatic slower.

Work is currently underway to improve the repetition rate of the adiabatic decelerator. Unfortunately, due to the cool down time of the ribbon after it has been heated, it is most effective at repetition rates less than 1 Hz. However, a source such as the heat pipe which is capable of reaching temperatures in excess of 1,000 K combined with a new high repetition rate decelerator would yield an even higher atomic flux. The ultimate repetition rate is limited to 1 kHz due to this being the limit of the Even-Lavie nozzle [62]. A Solid Edge rendering of the the slower used with the heat pipe as the entrainment source is shown in Fig. 4.1.

In addition to generating a larger number of cold atoms than laser cooling, entrainment is species independent. Because the noble gases used in supersonic beams do not typically react with other species [107], collisions during the entrainment process are elastic and the target species is collisionally

cooled. This is in stark contrast to laser cooling where particles are cooled by driving a two-level transition.

Since the majority of atoms do not have an easily accessible two-level transition and the complexity of molecules introduce rotational and vibrational degrees of freedom, laser cooling is only applicable to a select number of species [108, 109]. Even when laser cooling is applied to more complex species, many different repump lasers are required, making some experiments cost prohibitive [43]. Because entrainment is species independent, this new cooling technique is a more generally applicable method than laser cooling.

Chapter 5

Future Work

Future experiments hope to use the aforementioned entrainment techniques as the first step in a new cooling process. This new cooling process will translate the entrained atoms to rest using an atomic coilgun [72, 110], allowing new experiments which will benefit from higher cold atom flux than is currently achievable with laser cooling. In addition, by entraining two paramagnetic species into the same supersonic beam, both species are able to be translated to rest and trapped [111], at which point one species can be evaporatively cooled, sympathetically cooling the other species [112, 113].

By using sympathetic evaporative cooling in tandem with our new cooling technique, a wide variety of experimental opportunities become available, and many atomic physics labs will become more efficient. For example, a lab that only possesses a laser that is capable of addressing lithium is now able to perform experiments with any of the alkali metals as long as those metals are co-entrained with lithium. In addition to co-entraining different types of alkali atoms, it would also be feasible to co-entrain and trap two dissimilar species such as lithium and hydrogen. By evaporatively cooling lithium until

it is completely ejected from the trap, a BEC of hydrogen could be formed, allowing new fundamental studies of the hydrogen three body association rate [114]:

$$H + H + H \rightarrow H_2 + H. \tag{5.1}$$

In addition to studying the three body association rate of pure hydrogen which is of fundamental importance in determining the rate at which the first stars developed in the early universe [115, 116, 117], other astrophysically relevant reactions could also be studied. Because the primordial universe was primarily composed of hydrogen but also contained deuterium, helium, and lithium [118, 119, 120], reactions involving deuterium and lithium are also important in understanding our early universe [121, 122].

These reactions could be probed by repeating the hydrogen three body association reaction under conditions where a mixture of hydrogen and deuterium were entrained into the beam. In addition, reactions between lithium and hydrogen could be probed by stopping the evaporative cooling process before all lithium is ejected, leaving enough to observe reactions such as three body association of hydrogen where lithium carries away the excess energy:

$$H + H + Li \rightarrow H_2 + Li. \tag{5.2}$$

Future work which will require an even higher increase in atomic density is still feasible using this cooling technique. After trapping the entrained atoms, they can be compressed in phase-space using a technique called magneto-optical (MOP) cooling [40]. MOP cooling takes trapped atoms and compresses them in phase-space through velocity and spatially selective optical pump-

ing steps and magnetic kicks, effectively doubling the phase-space density with each step. Eventually, optical pumping will be limited by the rescattering of resonant photons [123], limiting MOP cooling to an atomic density of $10^{11} - 10^{12}$ atoms/cm^3.

By following MOP cooling with evaporative cooling, an ultra-cold and ultra-dense BEC can be formed. Since atom lithography has been limited by weak atom flux as well as magnetic lens aberrations [124], these larger condensates combined with an aberration-corrected pulsed magnetic lens will push the boundaries of atom lithography farther than has previously been realized [125].

Bibliography

[1] I. Newton, *Opticks* (London, 1704).

[2] M.-O. Mewes *et al.*, Phys. Rev. Lett. **78**, 582 (1997).

[3] I. Bloch, T. W. Hänsch, and T. Esslinger, Phys. Rev. Lett. **82**, 3008 (1999).

[4] A. D. Ludlow, M. M. Boyd, J. Ye, E. Peik, and P. O. Schmidt, Rev. Mod. Phys. **87**, 637 (2015).

[5] P. R. Berman, *Atom Interferometry* (Academic Press, 1997).

[6] P. Berg *et al.*, Phys. Rev. Lett. **114**, 063002 (2015).

[7] K. Hornberger, S. Gerlich, P. Haslinger, S. Nimmrichter, and M. Arndt, Rev. Mod. Phys. **84**, 157 (2012).

[8] S. Dimopoulos, P. W. Graham, J. H. Hogan, M. A. Kasevich, and S. Rajendran, Phys. Lett. B **678**, 37 (2009).

[9] M. R. Andrews *et al.*, Science **275**, 637 (1997).

[10] M. R. Matthews *et al.*, Phys. Rev. Lett. **83**, 2498 (1999).

[11] C. J. Pethick and H. Smith, *Bose-Einstein Condensation in Dilute Gases* (Cambridge, 2002).

[12] L. Fallani and A. Kastberg, EPL **110** (2015).

[13] A. J. Roncaglia, F. Cerisola, and J. P. Paz, Phys. Rev. Lett. **113**, 250601 (2014).

[14] H. J. Metcalf and P. van der Straten, *Laser Cooling and Trapping* (Springer, 2001).

[15] M. A. Kasevich, Science **298**, 1363 (2002).

[16] J. Kitching, S. Knappe, and E. A. Donley, IEEE Sens. J. **11**, 1749 (2011).

[17] M. A. Nielsen and I. L. Chuang, *Quantum Computation and Quantum Information* (Cambridge, 2004).

[18] C. J. Foot, *Atomic Physics* (Oxford University Press, 2005).

[19] B. J. Lester, N. Luick, A. M. Kaufman, C. M. Reynolds, and C. A. Regal, Phys. Rev. Lett. **115**, 073003 (2015).

[20] A. M. Nobili, Phys. Rev. A **93**, 023617 (2016).

[21] J. Williams, S. wey Chiow, N. Yu, and H. Mller, N. J. Phys. **18**, 025018 (2016).

[22] A. Loeb and D. Maoz, arXiv:1501.00996 [astro-ph.IM] (2015).

[23] S. Kolkowitz *et al.*, arXiv:1606.01859 [physics.atom-ph] (2016).

[24] Lord Rayleigh, Phil. Mag. **8**, 261 (1879).

[25] G. R. Fowles, *Introduction to Modern Optics* (Dover, 1989).

[26] Z. Liao, M. Al-Amri, and M. S. Zubairy, Phys. Rev. A **88**, 053809 (2013).

[27] L. A. Giannuzzi and F. A. Stevie, *Introduction to Focused Ion Beams: Instrumentation, Theory, Techniques, and Practice* (Springer, 2005).

[28] B. Knuffman, A. V. Steele, and J. J. McClelland, J. Appl. Phys. **114**, 044303 (2013).

[29] G. ten Haaf, S. H. W. Wouters, S. B. van der Geer, and E. J. D. Vredenbregt, J. Appl. Phys. **116**, 244301 (2014).

[30] A. Griesmaier, J. Werner, S. Hensler, J. Stuhler, and T. Pfau, Phys. Rev. Lett. **94**, 160401 (2005).

[31] W. Ketterle and N. J. Van Druten, Adv. At. Mol. Opt. Phy. **37**, 181 (1996).

[32] J. M. Doyle *et al.*, Physica B Condens. Matter **194-196**, 13 (1994).

[33] D. Egorov, T. Lahaye, W. Schöllkopf, B. Friedrich, and J. M. Doyle, Phys. Rev. A **66**, 043401 (2002).

[34] R. Rugango *et al.*, N. J. Phys. **17**, 035009 (2015).

[35] S. E. Maxwell *et al.*, Phys. Rev. Lett. **95**, 173201 (2005).

[36] Y. Castin, H. Wallis, and J. Dalibard, J. Opt. Soc. Am. B **6**, 2046 (1989).

[37] D. J. Wineland and H. Dehmelt, Bull. Am. Phys. Soc. **20**, 637 (1975).

[38] J. Dalibard and C. Cohen-Tannoudji, J. Opt. Soc. Am. B **6**, 2023 (1989).

[39] H. F. Hess, Phys. Rev. B **34**, 3476 (1986).

[40] M. G. Raizen, D. Budker, S. Rochester, J. Narevicius, and E. Narevicius, Opt. Lett. **39**, 4502 (2014).

[41] I. D. Setija *et al.*, Phys. Rev. Lett. **70**, 2257 (1993).

[42] M. Allegrini and E. Arimondo, Phys. Lett. A **172**, 271 (1993).

[43] E. S. Shuman, J. F. Barry, and D. DeMille, Nature **467**, 820 (2010).

[44] V. Zhelyazkova *et al.*, Phys. Rev. A **89**, 053416 (2014).

[45] I. Sivarajah, D. S. Goodman, J. E. Wells, F. A. Narducci, and W. W. Smith, Phys. Rev. A **86**, 063419 (2012).

[46] R. Rugango, A. T. Calvin, S. Janardan, G. Shu, and K. R. Brown, ChemPhysChem (to be published).

[47] P. Barletta, J. Tennyson, and P. F. Barker, N. J. Phys. **11**, 055029 (2009).

[48] N. R. Hutzler, H. Lu, and J. M. Doyle, Chem. Rev. **112**, 4803 (2012).

[49] R. deCarvalho *et al.*, Eur. Phys. J. D **7**, 289 (1999).

[50] T. C. Killian *et al.*, Phys. Rev. Lett. **81**, 3807 (1998).

[51] D. G. Fried *et al.*, Phys. Rev. Lett. **81**, 3811 (1998).

[52] R. I. Kaiser and A. G. Suits, Rev. Sci. Instrum. **66**, 5405 (1995).

[53] U. Even, Tel-Aviv University (private communication, 2015) .

[54] N. F. Ramsey, editor, *Molecular Beams* (Oxford, 1956).

[55] H. Pauly, *Atom, Molecule, and Cluster Beams I* (Springer, 2000).

[56] G. Scoles, editor, *Atomic and Molecular Beam Methods* (Oxford, 1988).

[57] M. Schnell and J. Kupper, Faraday Discuss. **150**, 33 (2011).

[58] E. Lavert-Ofir *et al.*, Nat. Chem. **6**, 332 (2014).

[59] Y. Shagam *et al.*, Nat. Chem. **7**, 921 (2015).

[60] U. Even, I. Al-Hroub, and J. Jortner, J. Chem. Phys. **115**, 2069 (2001).

[61] M. Mitsui, A. Nakajima, K. Kaya, and U. Even, J. Chem. Phys. **115**, 5707 (2001).

[62] H. Hillenkamp, S. Keinan, and U. Even, J. Chem. Phys. **118**, 8699 (2003).

[63] U. Even, Adv. Chem. **2014**, 636042 (2014).

[64] K. Luria, W. Christen, and U. Even, J. Phys. Chem. A **115**, 7362 (2011).

[65] W. Christen, K. Rademann, and U. Even, J. Phys. Chem. A **114**, 11189 (2010).

[66] S. Y. T. Van De Meerakker, H. L. Bethlem, and G. Meijer, Nat. Phys. **4**, 595 (2008).

[67] M. G. Raizen, Science **324**, 1403 (2009).

[68] N. Vanhaecke, U. Meier, M. Andrist, B. H. Meier, and F. Merkt, Phys. Rev. A **75**, 031402 (2007).

[69] E. Narevicius *et al.*, Phys. Rev. Lett. **100**, 093003 (2008).

[70] E. Narevicius *et al.*, Phys. Rev. A **77**, 051401 (2008).

[71] Y. Liu, S. Zhou, W. Zhong, P. Djuricanin, and T. Momose, Phys. Rev. A **91**, 021403 (2015).

[72] E. Lavert-Ofir *et al.*, Phys. Chem. Chem. Phys. **13**, 18948 (2011).

[73] D. Pentlehner *et al.*, Rev. Sci. Instrum. **80**, 043302 (2009).

[74] R. Radebaugh, J. Phys. Condens. Matter **21**, 164219 (2009).

[75] C. G. Townsend *et al.*, Phys. Rev. A **52**, 1423 (1995).

[76] U. Even, J. Jortner, D. Noy, N. Lavie, and M. Cossart-Magos, J. Chem. Phys. **112**, 8068 (2000).

[77] W. Christen, J. Chem. Phys. **139**, 154202 (2013).

[78] M. Guggemos, D. Heinrich, O. A. Herrera-Sancho, R. Blatt, and C. F. Roos, N. J. Phys. **17**, 103001 (2015).

[79] S. DePaul, D. Pullman, and B. Friedrich, J. Phys. Chem. **97**, 2167 (1993).

[80] I. Langmuir and K. H. Kingdon, Proc. R. Soc. A **107**, 61 (1925).

[81] J. B. Taylor, Phys. Rev. **35**, 375 (1930).

[82] R. Delhuille *et al.*, Rev. Sci. Instrum. **73**, 2249 (2002).

[83] J. Byskov-Nielsen, *Short-pulse laser ablation of metals*, Thesis, 2010.

[84] S. Nettesheim and R. Zenobi, Chem. Phys. Lett. **255**, 39 (1996).

[85] M. G. Kokish, M. R. Dietrich, and B. C. Odom, J. Phys. B: Mol. Opt. Phys. **49**, 035301 (2016).

[86] D. Bleiner and H. Altorfer, J. Anal. At. Spectrom. **20**, 754 (2005).

[87] R. Katzy, M. Singer, S. Izadnia, A. C. LaForge, and F. Stienkemeier, Rev. Sci. Instrum. **87**, 013105 (2016).

[88] L. V. Zhigilei, Appl. Phys. A **76**, 339 (2003).

[89] J. G. Lunney and R. Jordan, Appl. Surf. Sci. **127**, 941 (1998).

[90] B. N. Kozlov and B. A. Mamyrin, Tech. Phys. **44**, 1073 (1999).

[91] A. N. Nesmeyanov, *Vapour Pressure of the Elements* (Academic Press, 1963).

[92] M. E. Gehm, *Preparation of an optically-trapped degenerate gas of* ^6Li, Thesis, 2003.

[93] J. Fortagh, A. Grossman, T. W. Hansch, and C. Zimmermann, J. Appl. Phys. **84**, 6499 (1998).

[94] M. Borysow, *A High-Intensity Cold Atom Source*, Thesis, 2012.

[95] J. P. Gordon, H. J. Zeiger, and C. H. Townes, Phys. Rev. **99**, 1264 (1955).

[96] R. Senaratne *et al.*, Rev. Sci. Instrum. **86**, 023105 (2015).

[97] D. V. Schroeder, *An Introduction to Thermal Physics* (Addison Wesley Longman, 2000).

[98] R. G. DeVoe and C. Kurtsiefer, Phys. Rev. A **65**, 063407 (2002).

[99] G. Vittorini, K. Wright, K. R. Brown, A. W. Harter, and S. C. Doret, Rev. Sci. Instrum. **84**, 043112 (2013).

[100] R. D. Swenumson and U. Even, Rev. Sci. Instrum. **52**, 559 (1981).

[101] J. B. Boffard, M. E. Lagus, L. W. Anderson, and C. C. Lin, Rev. Sci. Instrum. **67**, 2738 (1996).

[102] D. Reay, P. Kew, and R. McGlen, *Heat Pipes: Theory, Design and Applications*, 6 ed. (Elsevier, 2013).

[103] G. K. Batchelor, *An Introduction to Fluid Dynamics* (Cambridge, 1967).

[104] M. Bober *et al.*, Meas. Sci. Technol. **26**, 075201 (2015).

[105] P. Hamilton *et al.*, Science **349**, 849 (2015).

[106] K. Van Tilburg, N. Leefer, L. Bougas, and D. Budker, Phys. Rev. Lett. **115**, 011802 (2015).

[107] P. Atkins and L. Jones, *Chemical Principles: the Quest for Insight*, 5 ed. (W. H. Freeman and Company, 2010).

[108] J. T. Bahns, W. C. Stwalley, and P. L. Gould, J. Chem. Phys. **104**, 9689 (1996).

[109] J. H. V. Nguyen *et al.*, N. J. Phys. **13**, 063023 (2011).

[110] E. Narevicius and M. G. Raizen, Chem. Rev. **112**, 4879 (2012).

[111] N. Akerman *et al.*, N. J. Phys. **17**, 065015 (2015).

[112] C. J. Myatt, E. A. Burt, R. W. Ghrist, E. A. Cornell, and C. E. Wieman, Phys. Rev. Lett. **78**, 586 (1997).

[113] F. Schreck *et al.*, Phys. Rev. A **64**, 011402 (2001).

[114] T. Morrison, *Hydrogen Studies Including Simulations for Three Body Association and Development of in-situ Silicon Passivation*, Thesis, 2015.

[115] V. Bromm, Rep. Prog. Phys. **76**, 112901 (2013).

[116] F. Palla, E. E. Salpeter, and S. W. Stahler, Astrophys. J. **271**, 632 (1983).

[117] M. J. Turk, T. Abel, and B. O'Shea, Science **325**, 601 (2009).

[118] D. Galli and F. Palla, Astron. Astrophys. **335**, 403 (1998).

[119] P. C. Stancil, S. Lepp, and A. Dalgarno, Astrophys. J. **509**, 1 (1998).

[120] M. Harwit and M. Spaans, Astrophys. J. **589**, 53 (2003).

[121] R. Martinazzo, G. F. Tantardini, E. Bodo, and F. A. Gianturco, J. Chem. Phys. **119**, 11241 (2003).

[122] D. Galli and F. Palla, Annu. Rev. Astron. Astrophys. **51**, 163 (2013).

[123] D. Tupa, L. W. Anderson, D. L. Huber, and J. E. Lawler, Phys. Rev. A **33**, 1045 (1986).

[124] R. J. Clark, T. R. Mazur, A. Libson, and M. G. Raizen, Appl. Phys. B-Lasers O. **103**, 547 (2011).

[125] R. Castillo-Garza, J. Gardner, S. Zisman, and M. G. Raizen, ACS Nano **7**, 4378 (2013).